



Munich Personal RePEc Archive

**Space-time patterns of rank concordance:
Local indicators of mobility association
with application to spatial income
inequality dynamics**

Rey, Sergio

Arizona State University

11 February 2016

Online at <https://mpra.ub.uni-muenchen.de/69480/>

MPRA Paper No. 69480, posted 12 Feb 2016 22:59 UTC

Space-Time Patterns of Rank Concordance: Local Indicators of Mobility Association with Application to Spatial Income Inequality Dynamics^{1 2}

SERGIO J. REY³

GeoDa Center for Geospatial Analysis and Computation

School of Geographical Sciences and Urban Planning

Arizona State University

srey@asu.edu

¹This is an Accepted Manuscript of an article published by Taylor & Francis Group in: *Annals of the Association of American Geographers*. DOI: 10.1080/24694452.2016.1151336.

²Code and data to reproduce the results of this article are available at <http://github.com/sjsrey/limaaag>.

³This research was supported in part by National Science Foundation Grant SES-1421935. Comments and suggestions by Dani Arribes-Bel, Janet Franklin, Wei Kang, Julia Koschinsky, Trisalyn Nelson, Myrna Sastre Gutiérrez, Levi Wolf, three anonymous referees, and the editor are greatly appreciated. Any remaining errors are mine alone.

Abstract

In the study of income inequality dynamics, the concept of exchange mobility plays a central role. Applications of classical rank correlation statistics have been used to assess the degree to which individual economies swap positions in the income distribution over time. These classic measures ignore the underlying geographical pattern of these rank changes. Rey (2004) introduced a spatial concordance statistic as an extension of Kendall's rank correlation statistic, a commonly employed measure of exchange mobility. This article suggests local forms of the global spatial concordance statistic: Local Indicators of Mobility Association (LIMA). The LIMA statistics allow for the decomposition of the global measure into the contributions associated with individual locations. They do so by considering the degree of concordance (stability) or discordance (exchange mobility) reflected within an economy's local spatial context. Different forms of the LIMAs derive from alternative expressions of the neighborhood and neighbor set. Additionally, the additive decomposition of the LIMAs permits the development of a meso-level analytic to examine whether the overall space-time concordance is driven by either interregional or intraregional concordance. The measures are illustrated in a case study that examines regional income dynamics in Mexico.

1. INTRODUCTION

Disparities in the levels of income between individuals in a society have long attracted attention across a variety of disciplines and have now assumed center stage in both policy and scientific circles (Stiglitz, 2012; Piketty, 2014). This attention reflects the concern that inequality can have negative impacts on social welfare and cohesion, as well as on economic growth (Cramer, 2003; Partridge, 1997).

Inequality at one point in time represents a snapshot of the path of the income distribution's evolution. That snapshot characterizes the outcomes of socioeconomic processes. While large inequalities in these outcomes draw much concern, it is important to keep in mind that the snapshot distribution is static and ignores any dynamics at work in the distribution's evolution. One response to this shortcoming has been the rise of the distribution dynamics literature (Quah, 1996b; Maasoumi et al., 2007) that adds a dynamic lens to the question of inequality. Here, measures of the external properties of the distribution, which include inequality indices, are tracked over time to provide a more comprehensive view of inequality dynamics.

The focus on the external properties of the distribution misses what some have argued is an equally important concept to inequality, and that is economic mobility (Fields, 2010; Hammond and Thompson, 2006; Schorrocks, 1978). Consider two societies with equally high levels of inequality and similar external distribution dynamics such that dispersion in the distribution is increasing over time. From this perspective the two systems would seem indistinguishable regarding their respective inequality dynamics. Yet the welfare of individuals from each of these societies would be different if one of the systems displayed higher income mobility than the other, since the opportunities for changing one's position in the distribution would be improved.

Economic mobility is, however, less clearly defined than economic inequality as a number of different types of mobility have been described. One distinction is between absolute and relative mobility. When individuals move away from their initial levels of income in a distribution absolute mobility occurs. Relative mobility is more of a re-ranking phenomena whereby the movement of an observation in the distribution is considered with respect to the positions of other observations in the distribution (Formby et al., 2004). In other words, relative mobility occurs when the ordinal positions change over time, whereas absolute mobility reflects changes in the cardinal positions. Absolute and relative mobility are sometimes referred to as structural and exchange mobility

(Maasoumi, 1998).

The income inequality literature has preceded the mobility literature in identifying the need for, and incorporating, a spatial perspective. This reflects the recognition that income disparities between countries are the focus of the literature despite often being smaller than disparities within countries (The Economist, 2011). From a policy perspective, regional disparities have motivated for the establishment of programs targeting economic development (Jalan and Ravallion, 1998; Bigman and Srinivasan, 2002). A related question is how intergenerational income mobility may vary depending upon geographical context (Chetty et al., 2014). On the methodological front the dominant theme is work on spatial inequality decomposition where economies within a national system are placed into mutually exclusive and exhaustive regions and then overall inequality is decomposed into that due to disparities between economies from different regions and that due to disparities among economies within each of the regions. A common finding across the large corpus of these studies is that within region inequality tends to dominate inequality between regions (Shorrocks and Wan, 2005, p. 68).

While the inequality literature has taken the spatial turn sooner than the mobility literature has, there have been some recent extensions of distributional dynamic approaches that incorporate spatial considerations. Discrete Markov chains (Quah, 1996a; Magrini, 1999) and rank correlation statistics (Webber et al., 2005; Cuadrado-Roura, 2009) have played a central role in this regard. The discrete Markov chain framework has been enhanced to allow for regional conditioning of the transitional probabilities using so-called spatial Markov chains (Rey, 2001; Le Gallo, 2004). A second extension has been the development of a space-time version of a rank correlation measure of income mobility (Rey, 2004). Spatio-temporal rank correlation examines the extent to which the overall mobility, or changes in the ranks of economies, displays a geographical pattern or not.

These spatial extensions to mobility measures are required to assess the extent to which spatial dependence and/or spatial heterogeneity are present. Non-spatial approaches to inference regarding income mobility indices are based on the assumption of independence (Schluter, 1998; Formby et al., 2004), and thus their use in a spatial context is problematic. At the same time, existing spatial mobility measures are global in nature. That is, they report on the extent of spatial dependence and heterogeneity in the overall distribution, yet are silent on the patterns of local mobility. Local mobility may reflect hot spots of spatial change, or cohesion, in the distributional

dynamics in the sense that the movements of an individual region in the income distribution over time are related to those of its neighboring regions.

In this article I extend Rey (2004) to develop a family of local indicators for mobility analysis (LIMA). These allow for a decomposition of the global measure of spatial rank concordance into spatially explicit contributions associated with each individual regional observation. Different forms of the LIMA are suggested that allow for alternative representations of regional context. As a complement to the local measures, I also suggest that the additive nature of the decomposition of the LIMAs permits the development of meso-scale measures of interregional mobility that can be used to examine the distinction between interregional and intraregional income mobility dynamics, analogous to the approach used in the interregional inequality literature (Kanbur and Venables, 2005). I also propose approaches to inference for the LIMAs and their interregional decomposition.¹

In the remainder of the article I first revisit the global indicator of spatial concordance that serves as the foundation for the derivation of the local measures (Section 2). Next a family of local indicators for mobility analysis are presented along with a meso-scale level indicator that considers the concepts of interregional and intraregional distributional mobility (Section 3). These measures are examined in an empirical application of Mexican state per capita gross domestic product dynamics over the period 1940-2000 (Section 4). I close the article with some concluding comments and the identification of future research directions (Section 5).

2. GLOBAL INDICATORS OF MOBILITY ASSOCIATION

The departure point for the development of spatial measures of mobility is the general rank correlation coefficient originally suggested by Kendall (1962):

$$\tau(g, f) = \frac{\sum_{i=0}^{n-2} \sum_{j=i+1}^{n-1} \text{sgn}(f_i - f_j) \text{sgn}(g_i - g_j)}{n(n-1)/2} = \frac{c - d}{n(n-1)/2} \quad (1)$$

where f and g are variables with observations over $i = 1, 2, \dots, n$ units. The numerator reflects the net-concordance between all pairs of observations on these two variables, where c is the number

¹The focus in this paper is on new methods for the analysis of regional income inequality dynamics. The literatures on inequality in personal income distributions, where the observational unit is an individual, and regional income inequality, where the observational unit is a regional economy, are largely separate ones. For a recent examination of the potential linkages between these two literatures see Rey (2016).

of concordant pairs, and d the number of discordant pairs. As a correlation measure the range is $-1 \leq \tau(g, f) \leq 1$. For small samples the exact distribution of $\tau(g, f)$ can be obtained through full enumeration under the null of rank independence. Asymptotically $\tau(g, f)$ has a normal distribution with mean 0 and variance $\frac{4n+10}{9n(n+1)}$.

In the convergence literature the two variables are defined as incomes in an initial ($f_i = y_{i,t_0}$) and ending period ($g_i = y_{i,t_1}$), respectively. Given the range of $\tau(g, f)$ the sign of the coefficient matters when considering mobility or rank changes in the distribution. Thus a derived measure of mobility could be defined as:

$$M = \frac{\tau(g, f) - 1}{-2} \quad (2)$$

with $0 \leq M \leq 1$. Economies with larger values of M would display greater distributional mixing over a given period relative to those economies with lower values of M . Note that having $\tau(g, f) = 0$ does not imply the absence of rank mobility, rather a value of $\tau(g, f) = 1$ would.

2.1. Spatial Decomposition of Rank Mobility

In Rey (2004) a spatial version of Kendall's statistic was based on a decomposition of the pairs into those that are geographical neighbors and those that are not. Define the matrix S with elements $s_{i,j} = 1$ if observations i, j are concordant, $s_{i,j} = -1$ if i, j are discordant, and $s_{i,j} = 0$ otherwise, then equation (1) can be redefined using:

$$c - d = \frac{1}{2} \sum_i \sum_j s_{i,j}$$

to give:

$$\tau(g, f) = \frac{\iota' S \iota}{n(n-1)} \quad (3)$$

with ι the $(n \times 1)$ unit vector. Let W denote a binary spatial weights matrix with elements $w_{i,j} = 1$ if observations i and j are geographical neighbors, 0 otherwise, and $\bar{W} = \iota \iota' - W - I$, we can then define the matrix S :

$$S = W \circ S + \bar{W} \circ S \quad (4)$$

where \circ is the Hadamard product.

Noting that $l'(W + \bar{W})_t = n(n - 1)$ we have:

$$\tau(g, f) = \frac{l'(W \circ S + \bar{W} \circ S)_t}{l'(W + \bar{W})_t} = \frac{l'(W \circ S)_t + l'(\bar{W} \circ S)_t}{l'(W + \bar{W})_t} \quad (5)$$

or, equivalently:

$$\tau(g, f) = \frac{l'W_t}{l'(W + \bar{W})_t} \frac{l'(W \circ S)_t}{l'W_t} + \frac{l'\bar{W}_t}{l'(W + \bar{W})_t} \frac{l'(\bar{W} \circ S)_t}{l'\bar{W}_t} = \psi \tau_w(g, f) + (1 - \psi) \tau_{\bar{w}}(g, f) \quad (6)$$

which has the classic rank correlation statistic as a weighted average of the rank correlation for neighboring pairs and that for the non-neighbor pairs with $\psi = \frac{l'W_t}{l'(W + \bar{W})_t}$.

The decomposition determines whether the classic measure masks different correlation patterns between the two pair sets: neighboring and non-neighboring. Inference on this question can be based on random spatial permutations of the attributes to develop a distribution for τ_w under the null of spatial homogeneity in the correlation patterns between the neighbor and non-neighbor pairs. As this statistic yields a single value for the amount of rank mobility in the entire distribution over two points in time it can be considered a *Global Indicator of Mobility Association* (GIMA). Given the relationship between the traditional τ from (1) and the derived mobility index in (2), a spatial mobility measure can be defined as:

$$M_W = \frac{\tau_W - 1}{-2}. \quad (7)$$

This also allows for an additive decomposition of overall mobility:

$$M = \psi M_W + (1 - \psi) M_{\bar{W}}. \quad (8)$$

To illustrate this GIMA consider Figure 1 which displays the spatial distribution of ranks on a map of 16 regularly sized regional units at period t_0 (Figure 1a) and period t_1 (Figure 1b). Also shown is a partition of the units into four regimes (Figure 1c) which can be used to operationalize neighbors using so called block weights (Anselin and Rey, 2014, p. 37) such that $W_{i,j} = 1$ if $R(i) = R(j)$, otherwise $W_{i,j} = 0$, where R is a function that maps an observation to its regime.

[Figure 1 about here.]

The classic rank correlation statistic takes on a value of $\tau = 0.90$ for this example. Of the 120

(i.e., $16 \cdot 15 / 2$) pairs, 114 are concordant over the two periods, while 6 pairs are discordant. Close inspection of the rank distribution in the second period reveals that the 6 discordant pairs are contained in regime 3. The spatially focused nature of the discordance is reflected in the lower rank correlation value for the neighbors, $\tau_W = 0.50$. Moreover, all of the non-neighbor pairs are concordant given $\tau_{\bar{W}} = 1.00$. Based on 999 random permutations, the spatial τ_w is significant at $p = 0.001$ indicating different concordance relationships are found between the neighboring and non-neighboring pairs.

A second example can be seen in Figure 2. Here the rank distribution in the first period is the same as the previous case but the rank distribution has changed in a different fashion (Figure 2b). Members of regime 1 leapfrog those in regime 0, and those in regime 2 now swap ranks with those in regime 3. As a result, the overall rank correlation drops $\tau = 0.467$, however the spatial rank correlation measure is at $\tau_W = 1.0$ as the ordinal relations for all neighbor pairs remain constant over the two periods. Based on 999 random spatial permutations of the observations on both variables jointly, the p-value for the τ_W is 0.002. Because the same spatial permutation is applied to both time periods, the overall amount of mobility will be maintained across each of the permutations.

[Figure 2 about here.]

2.2. Space-Time Concordances and Spatial Autocorrelation

When cross-sectional observations are available over multiple time periods, a common analytical strategy is to apply a global measure of spatial autocorrelation to explore how spatial dependence may be evolving overtime (Rey and Montouri, 1999, p. 146). It is important to note that space-time concordance, as measured using the spatial τ_W above, focuses on different properties of the changes in a spatial distribution from those offered by existing global spatial autocorrelation measures applied in a space-time context. Returning to the example in Figure 1, the application of Moran's I using the regime weights yields identical values for the global spatial autocorrelation statistic in both periods, despite the change in the spatial distribution. By contrast, we see that the classic τ (0.90) and the spatial τ_W (0.50) now reflect lower concordance between the spatially neighboring pairs than what holds between non-neighbor pairs.

If the spatial weights are redefined to use contiguity weights based on the rook criterion, the

level of spatial autocorrelation declines slightly in the second period (0.775 vs. 0.740) whereas the global classic τ remains at 0.90 and the spatial τ_W is now 0.667. While the latter has increased in value relative to the case when the block weights were used, it remains statistically significant pointing to different concordance relations for the neighboring and non-neighboring pairs.

These two examples illustrate that space-time concordance and changes in spatial autocorrelation over time are not identical. The space-time concordance measures consider how the pairwise ordinal associations between neighboring values evolve over time, while the difference in the global autocorrelation statistic captures how pairwise interval associations change between time periods. The two measures should be thought of as complements and not substitutes because they capture different aspects of spatial distribution dynamics. This will be explored more fully below.

3. A FAMILY OF LOCAL INDICATORS OF MOBILITY ASSOCIATION

The complementary nature of the global space-time mobility measure and the global autocorrelation also serves as the inspiration for the development of local indicators for mobility analysis (LIMA). The LIMAs can be viewed as counterparts to the local indicators of spatial association (LISA) suggested by Anselin (1995).

3.1. Local Concordance

A number of different local space-time concordance measures can be derived from the global measures. The first is a local version of the classic τ :

$$\tau_r(y_t, y_{t+1}) = \frac{\sum_{b \neq r} \text{sgn}(y_{r,t} - y_{b,t}) \text{sgn}(y_{r,t+1} - y_{b,t+1})}{(n-1)} = \frac{c_r - d_r}{(n-1)} = \frac{l'_r S t}{n-1} \quad (9)$$

where l_r is an $(n \times 1)$ vector with a 1 in position r and 0 elsewhere, y_t and y_{t+1} are $(n \times 1)$ vectors of regional incomes in periods t and $t+1$. The numerator is the sum of row r of S from (4). Normalizing by $n-1$ provides a local net-concordance indicator for location r . The local concordance measure provides an indication of the contribution of location r 's rank changes to the overall level of space-time mobility. This is because the classic measure can be decomposed into

the local components given that:

$$\sum_r \tau_r = \sum_r \frac{\sum_b s_{r,b}}{(n-1)} \quad (10)$$

$$= \frac{1}{n-1} \sum_r \sum_b s_{r,b} \quad (11)$$

$$= \frac{1}{n-1} n(n-1)\tau \quad (12)$$

or

$$\tau = \frac{1}{n} \sum_r \tau_r. \quad (13)$$

3.2. LISA Concordance

Although the measure from (9) is location specific, it is not a spatial statistic because local context is not taken into account. Rather, the local concordance measure for r reports on how that location's rank has moved relative to the ranks at *all other locations* over the two periods. No distinction is drawn between the locations that neighbor r and those that do not. To introduce local spatial context, a LISA could be applied to the collection of τ_r values:

$$I_{\tau,r} = \left(\frac{z_r}{m_2} \right) \sum_b w_{r,b} z_b \quad (14)$$

where $z_r = \tau_r - \tau$, and $m_2 = \sum_r \frac{z_r^2}{n}$. The LISA compares the local concordance measure for each neighbor against the same measure for the focal unit.

3.3. Neighbor Set LIMA

Applying a LISA to the local concordance measure allows for the investigation of whether the spatial distribution of rank changes is random, or not, over two periods. What it does not do, however, is consider the local concordance relationships between a focal unit and its neighbors. The second LIMA explicitly considers concordance between neighboring pairs of observations:

$$\tau_r = \psi_r \tau_{W,r} + (1 - \psi_r) \tau_{\bar{W},r} \quad (15)$$

with $\psi_r = \frac{\sum_b w_{r,b}}{n-1}$, $\tau_{W,r} = \frac{\sum_b w_{r,b} s_{r,b}}{\sum_b w_{r,b}}$, and $\tau_{\bar{W},r} = \frac{\sum_b \bar{w}_{r,b} s_{r,b}}{\sum_b \bar{w}_{r,b}}$. This decomposes the local concordance measure from (9) into neighbor and non-neighbor components. Inference on the neighbor component could be based on conditional permutations of the observations over the two time periods. For each permutation the only component of $\psi_r \frac{\sum_b w_{r,b} s_{r,b}}{\sum_b w_{r,b}}$ that will be of interest is $\sum_b w_{r,b} s_{r,b}$ as the other terms will remain constant over the permutations.

Thus, our second LIMA is defined as:

$$\tilde{\tau}_r = \frac{\sum_b w_{r,b} s_{r,b}}{\sum_b w_{r,b}}. \quad (16)$$

Recall that the global measure can be decomposed into the global neighbor and global non-neighbor components:

$$\tau = \frac{l'W_l}{l'(W + \bar{W})_l} \frac{l'(W \circ S)_l}{l'W_l} + \frac{l'\bar{W}_l}{l'(W + \bar{W})_l} \frac{l'(\bar{W} \circ S)_l}{l'\bar{W}_l} = \psi \tau_w + (1 - \psi) \tau_{\bar{w}}$$

and isolating on the global neighbor component: $\psi \tau_w$ we have:

$$\tau_w = \sum_r \psi_r \tau_{w,r} \quad (17)$$

$$= \sum_r \frac{\sum_b w_{r,b}}{\sum_r \sum_b w_{r,b}} \tau_{w,r} \quad (18)$$

$$= \sum_r \frac{\sum_b w_{r,b}}{\sum_r \sum_b w_{r,b}} \frac{\sum_b w_{r,b} s_{r,b}}{\sum_b w_{r,b}} \quad (19)$$

$$= \sum_r \frac{\sum_b w_{r,b} s_{r,b}}{\sum_r \sum_b w_{r,b}} \quad (20)$$

$$= \frac{\sum_r \sum_b w_{r,b} s_{r,b}}{\sum_r \sum_b w_{r,b}} \quad (21)$$

Unlike the decomposition of τ in (13) where the local components have equal weights, here the decomposition of τ_w uses a weighted average of the local $\tau_{w,r}$ where the weights are a function of the number of neighbors at each location.

3.4. Neighborhood Set LIMA

One issue with the form of $\tilde{\tau}_r$ in (16) is that focusing on only the spatial component as the ratio of net-concordance for unit r over the number of its neighbors may limit the range of values that

can be observed. For example, in a regular lattice under rook contiguity the maximum number of neighbors for any unit would be 4. This would define the denominator in $\tau_{w,r} = \frac{\sum_b w_{r,b} s_{r,b}}{\sum_b w_{r,b}}$. In this case, the numerator could take on only one of 5 possible values [0,4] and this will result in the distribution of the $\tau_{w,r}$ having a limited range which in turn may make detection of significant locations difficult.

One way to address this is to extend the local concordance measure to consider a focal unit's *neighborhood set*:

$$\tilde{\tau}_r = \frac{\sum_{a \in H_r} \sum_{b \in H_r/a} s_{a,b}}{|H_r|(|H_r| - 1)} \quad (22)$$

where $H_r := G_r \cup \{r\}$ and $G_r := \{b : w_{r,b} = 1\}$. The neighborhood set, H_r , allows for a larger number of pairs to determine the local concordance indicator at focal unit r . Now in addition to the concordance relations between r and its neighbors, the concordance between *all the pairs* within r 's neighborhood set are also included. Continuing with an internal cell for the rook case on a regular lattice gives $|H_r| = 5$ and the denominator in (22) becomes 20. Note that the pairs are counted twice in both the numerator and denominator, so the numerator can now take on 11 unique values: $(0, 2, \dots, 18, 20)$ increasing the range of the distribution for this LIMA relative to the previous one. Inference on the LIMA in (22) can rely on conditional spatial permutations.

The comparison of the local neighbor concordance measure to the local concordance measure could also be applied to the extended neighborhood set based LIMA:

$$\tau'_r = \omega_{H,r} \frac{\sum_{a \in H_r} \sum_{b \in H_r/a} s_{a,b}}{|H_r|(|H_r| - 1)} + (1 - \omega_{H,r}) \frac{\sum_{a \in \tilde{H}_r} \sum_{b \in \tilde{H}_r/a} s_{a,b}}{|\tilde{H}_r|(|\tilde{H}_r| - 1)} \quad (23)$$

where $\tilde{H}_r := N \setminus G_r$ and $N := \{1, 2, 3, \dots, n\}$, and $\omega_{H,r} = \frac{|H_r|(|H_r| - 1)}{n(n-1)}$.

The prime indicates that the form of the LIMA in (23) is not identical the one defined in (15). The key distinction between the two derives from the definitions of the neighbor and neighborhood sets. In the first LIMA the neighbor set is used to compare the concordance of the focal unit with that of each of its neighbors. In the final LIMA, the concordance between all pairs of units belonging to the neighborhood set of the focal unit is used.

3.5. Interregional Mobility Decomposition

The use of block weights when partitioning spatial observations into regimes also facilitates the decomposition of overall mobility into two components: intraregional mobility and interregional mobility. More formally, define P as a regional aggregation matrix of dimension $K \times n$ with K equal to the number of regions. This is used to define an exhaustive and mutually exclusive partition of the areas into K regions such that $P_{k,i} = 1$ if $i \in k$ otherwise $P_{k,i} = 0$, and $\sum_k P_{k,i} = 1 \forall i$. Using this aggregation matrix, the local concordance measures can be aggregated to consider concordance between and within the regimes:

$$\tau = \frac{\iota_K' P(W \circ S) P' \iota_K}{\iota_K' D \iota_K} + \frac{\iota_K' P(\bar{W} \circ S) P' \iota_K}{\iota_K' D \iota_K} \quad (24)$$

where $D = PWP' + P\bar{W}P'$, and ι_K is a $K \times 1$ unit vector. The first term on the right hand side of (24) is a function of the amount of intraregional concordance, while the second is driven by concordance between members of different regions, or interregional concordance.

Returning to the first example from Figure 1, the matrix P takes the following form:

$$P = \begin{bmatrix} 1 & 1 & 0 & 0 & 1 & 1 & 0 & 0 & 0 & 0 & 0 & 0 & 0 & 0 & 0 \\ 0 & 0 & 1 & 1 & 0 & 0 & 1 & 1 & 0 & 0 & 0 & 0 & 0 & 0 & 0 \\ 0 & 0 & 0 & 0 & 0 & 0 & 0 & 0 & 1 & 1 & 0 & 0 & 1 & 1 & 0 \\ 0 & 0 & 0 & 0 & 0 & 0 & 0 & 0 & 0 & 0 & 1 & 1 & 0 & 0 & 1 \end{bmatrix}$$

In this example, interregional mobility is at its theoretical minimum ($M_{\bar{W}} = 0$) as the ordinal relations involving pairs of observations from disjoint regimes remain unchanged over the two periods. Consequently, the low overall mobility ($M = 0.05$) is due to mobility in the intraregional component associated with rank changes within regime 3 giving $M_w = 0.25$. Recall that for this example the global $\tau = 0.90$, which, when using the decomposition in (24) yields:

$$\tau = 0.10 + 0.80 = 0.90 \quad (25)$$

with the high intraregional mobility being reflected in the low relative intraregional concordance in term 1, and the low interregional mobility seen in the high relative concordance of term 2. In

the second example there is a greater amount of overall mobility ($M = 0.267$) and this is driven by the inter-regime component ($M_{\bar{W}} = 0.334$), whereas the intra-regime mobility is at its theoretical minimum: $M_w = 0$. In this case the global τ is decomposed using (24) as:

$$\tau = 0.267 + 0.200 = 0.467. \quad (26)$$

The decomposition in (24) is a scalar decomposition, which can be shown to be equivalent to the GIMA from (6). However, the decomposition can also be unpacked in matrix form as:

$$T = \frac{P(W \circ S)P'}{D} + \frac{P(\bar{W} \circ S)P'}{D} \quad (27)$$

where T is now a $K \times K$ concordance matrix with diagonal elements measuring concordance between units within a regime and the off-diagonal elements denoting concordance between observations from a specific pair of different regimes. The $K \times K$ matrix D reports twice the number of pairwise comparisons for either the specific intraregional (along the diagonal) or interregional comparison (off-diagonal elements). For the first example, we have:

$$P(W \circ S)P' = \begin{bmatrix} 12 & 0 & 0 & 0 \\ 0 & 12 & 0 & 0 \\ 0 & 0 & 12 & 0 \\ 0 & 0 & 0 & -12 \end{bmatrix},$$

$$P(\bar{W} \circ S)P' = \begin{bmatrix} 0 & 16 & 16 & 16 \\ 16 & 0 & 16 & 16 \\ 16 & 16 & 0 & 16 \\ 16 & 16 & 16 & 0 \end{bmatrix},$$

and the matrix D is:

$$D = \begin{bmatrix} 12 & 16 & 16 & 16 \\ 16 & 12 & 16 & 16 \\ 16 & 16 & 12 & 16 \\ 16 & 16 & 16 & 12 \end{bmatrix}.$$

As a result, the matrix T is:

$$T = \begin{bmatrix} 1 & 1 & 1 & 1 \\ 1 & 1 & 1 & 1 \\ 1 & 1 & 1 & 1 \\ 1 & 1 & 1 & -1 \end{bmatrix}.$$

For the second example we have:

$$T = \begin{bmatrix} 1 & -1 & 1 & 1 \\ -1 & 1 & 1 & 1 \\ 1 & 1 & 1 & -1 \\ 1 & 1 & -1 & 1 \end{bmatrix}.$$

4. EMPIRICAL ILLUSTRATION: SPATIAL INCOME DYNAMICS IN MEXICO 1940-2000

As an initial demonstration of the use of the LIMA measures, data from a previous study by Rey and Sastré-Gutiérrez (2010) on regional income dynamics in the 32 Mexican states over the decades of 1940-2000 is employed. Figure 3 illustrates the changing spatial distribution of gross regional domestic product per capita using quintile classifications for each decade.² The well-known north-south divide (Aroca et al., 2005) in the Mexican space economy is evident throughout all decades. At the same time, there is visual evidence that states can move in and out of quintiles over time which, by definition, is evidence of rank mobility.

Figure 4 contains the “spaghetti plot” for Mexican relative per capita gross state product over 1940-2000. Here the state values are normalized to the mean each decade. The name of the plot is motivated by the reasoning put forth by Beenstock and Felsenstein (2007) who coined the phrase “spaghetti convergence” which combines both absolute and relative mobility. The state names are

²Figure 6a contains a map of the Mexican states.

listed in descending ranks for the first and last decade.

The distribution displays greater dispersion for the high income states relative to the narrower concentration of time series at the bottom of the distribution. Despite the gaps at the top end of the distribution there is still evidence of positional leapfrogging, and in some instances the movements are fairly dramatic in both downward and upward directions. Campeche and Mexico experience the largest upwards movements in the distribution climbing 20 and 9 ranks, respectively. The largest downward moves in the distribution are those of Durango and Nayarit, dropping 13 and 10 ranks over the period.

The visual complexity of the distributional mixing makes more detailed interpretation difficult as the linear ordering of the ranks precludes any consideration of the geographical relationships between the rank movements of the states. Figure 5 displays the spatial distribution of positional change alongside the cumulative sum of absolute rank change over the entire 60 year period. The latter measures the overall volatility in the rank movements of individual states. There is no relationship between the volatility in a state's position decade-to-decade and the magnitude of the positional change in the income distribution over this period ($\rho = 0.30$, $p = 0.10$). The two measures also display distinct spatial patterns, as the volatility of ranks is highly spatially autocorrelated ($I = 0.33$, $p = 0.01$), while the end-point change is spatially random ($I = 0.03$, $p = 0.29$).³ A more detailed spatiotemporal analysis of the rank dynamics necessitates the application of the LIMAs as shown in the following sections.

[Figure 3 about here.]

[Figure 4 about here.]

[Figure 5 about here.]

[Figure 6 about here.]

4.1. Global Autocorrelation and Global Mobility

Table 1 summarizes the global measures of spatial autocorrelation and rank concordance over the 60 year period. In both cases the spatial weights are defined using block weights reflecting the

³Spatial autocorrelation is measured with Moran's I and a row-standardized Queen contiguity matrix using the PySAL library (Rey and Anselin, 2007).

regions defined in Figure 6b. The complementary nature of the two statistics is reflected in the significant spatial rank mobility found in the first three decades of the sample, as the degree of rank concordance between neighboring pairs is significantly lower than what would be expected under spatial randomness of rank changes. Coexisting with this rank mobility are spatially random incomes in the first two decades with spatial autocorrelation becoming significant in 1960. From 1970 forward the pattern switches to rank concordance that does not depart from spatial randomness, in the sense that the concordance pattern for neighboring states is not distinguished from that between states that are not neighbors, while the levels of income remains spatially autocorrelated throughout 1970-2000.

[Table 1 about here.]

4.2. LIMAs

Local Concordance τ_i : Table 2 reports the location specific τ_i values for each 10-year transitional period, along with the results of a local indicator of spatial association for each value. The τ_i values associated with a significant LISA are indicated in bold. Recall that the τ_i reports the concordance between a specific state's income rank and the rest of the system, while the LISA asks if these τ_i values are locally clustered in space.

With regard to the τ_i values, concordance is the dominant pattern. This is seen, for example, in Distro Federal for the 1940-50 period over which it does not swap ranks with any of the other states (also see Figure 4). There are some exceptions, however, as both Aguascalientes and Queretaro have negative τ_i values in the first transitional period, indicating that they are sources of rank change in the distribution. As was noted above, Campeche experienced the greatest upward movement in the rank distribution over the entire period, yet examination of Table 2 reveals that much of this movement was concentrated in the 1980-90 period as reflected in the strong negative τ_i . The local τ_i values can also vary in sign and magnitude for a given state over time. For example, Campeche's strong negative value in the 1980-90 period is bracketed by strong concordance values, and a similar pattern can be seen for the state of Tabasco.

The local spatial association pattern of these state concordance values is also complex. The bold values indicate significant LISA values for the specific τ_i but the nature of those spatial relationships varies over the states in question. Significant LISAs are found for the negative τ_i

values in 1940-50 for Aguascalientes and Queretaro, while the remaining significant LISAs are all associated with positive τ_i values for the focal state. It is important to note; that, in the former case the significant LISAs are pointing to spatial outliers - the strong negative concordance values for Aguascalientes and Queretaro are significantly different from the concordance values in their neighboring states. For other significant LISAs the pattern is of spatial value similarity for the state-specific concordance values, whether those concordance values are strongly, or weakly, positive. This indicates that, relative to the entire spatial distribution, these states generally hold their rank positions. It does not necessarily imply that the concordance relationships between the neighboring pairs are stable, however.

[Table 2 about here.]

Neighbor set $\tilde{\tau}_i$: Table 3 reports the values for the version of the LIMA based on the neighbor set. Here the question is whether the concordance relationship between the focal state and its neighbors is different from what could be expected from randomly distributed rank changes. Inference is based on conditional randomization for each state under the null. That is, the sampling distribution for the local $\tilde{\tau}_i$ is obtained by randomly selecting n_i neighbors from the set of n that excludes i and recalculating the statistic. This process is repeated 99 times for each state, and pseudo p-values are obtained by comparing the observed statistic to this conditional distribution under the null.

There are a number of interesting patterns that emerge from the table. The value for the LIMA in Campeche is significant in four of the six transitional periods, three of which show concordance while one displays discordance with its neighbors. In the discordant period Campeche has swapped positions with all of its neighbors, again reflecting the period where it climbed up the income distribution in rapid fashion. Thus, not only did it pass states that were not its geographical neighbors (as was seen in the previous table), it also leapfrogged its geographical neighbors.

Another interesting case of local spatial dynamics is seen in Oaxaca situated in the poverty belt of Mexico's southern states. While the received wisdom is that southern states lag behind the rest of the country, what has not been recognized is the complexity of the local spatial dynamics within this region. The stability in the local rank positions from 1960-90 is clearly seen, yet there are signs that local rank mobility can increase over some decades, and in the case of 1950-60 radically so.

Alongside these cases of spatial flux we see pockets of local rank stability, and, in one instance,

dominance. Distrito Federal maintains its position relative to its neighbors during each of the transitional periods. However, its local value is significant in four, but not all, of the six transitions. Even though the observed values are the same in all six years, the distribution of the local statistic under the null is sensitive to the overall amount of concordance in the rank distribution over a specific transition period.

[Table 3 about here.]

Neighborhood Set $\tilde{\tau}_i$: Table 4 reports the values for the version of the LIMA based on the neighborhood set. Now the question is if the concordance relationships for a subset of states, defined as the focal state and its neighbors, is different from what would be expected from randomly distributed rank changes. In contrast to the previous LIMA where the concordance relationship is viewed as a one-to-many (i.e., focal to each of its neighbors), here the local concordance value is based on a many-to-many relationship. That is, the pairwise concordance relations are measured for all pairs of states belonging to a focal state's neighborhood set. Inference is again based on conditional random permutations for each state.

A comparison of Tables 4 and 3 reveals a number of important differences in the local concordance measures, as well as a few similarities. An important distinction is the non-negativity of the local values for $\tilde{\tau}_i$ in contrast to more instances of local discordance reported in Table 3. One clear example of this is Campeche which goes from total local discordance in 1980-90 according to $\tilde{\tau}_i$, to a local concordance value of $\tilde{\tau}_i = 0$ during the same period when using the neighborhood set basis. This implies that while Campeche leapfrogged all of its neighbors during this transition period, the pattern of pairwise concordance between each of its neighbors was a more mixed one with the number of concordant and discordant pairs counterbalancing in Campeche's neighborhood set. An explanation for the dominance of positive values for neighborhood set LIMA in Table 4 is that the transitions are for a short 10-year period and the number of concordance pairwise relations for members within a neighborhood set dominates the fewer instances of pairwise discordance in the set.

In contrast to the case of Campeche, the values of the two types of LIMAs are identical for Distrito Federal, pointing to absolute concordance between itself and its neighbors, but also between all pairs of Distrito Federal's neighbors. There is, however, a difference in the temporal pattern of the significance of the two LIMAs. Again, this reflects the different nature of the

neighborhood set and the neighbor set constructs that define the two statistics.

It also important to note that the values for this second LIMA will be identical for all members of a neighborhood set given that block weights are used. What may vary over the members of the neighborhood set is the significance of the statistic because the permutations are conditional upon the focal state under consideration. This is seen in the case of Mexico and Distrito Federal which comprise the capital region.

The two sets of LIMAs thus provide complementary views on the local spatial dynamics, the former yielding insights as to a focal state's concordance relationships with its neighbors and the latter describing the regional concordance dynamics surrounding the focal state.

[Table 4 about here.]

4.3. Interregional and Intra-regional Mobility Decomposition

The results of applying the interregional concordance decomposition are reported in Table 5. The diagonal elements report the amount of intra-regional concordance in state incomes between 1940 and 2000, while the off-diagonal elements measure interregional concordance. Bold values indicate statistical significance at $p = 0.05$, where inference is based on random spatial permutations of the state incomes. It is important to note that the global level of rank concordance remains constant over the permutations. Thus, the null hypothesis here is whether the interregional or intra-regional concordance observed is significantly different from what would be expected if income mobility were random in its spatial distribution.

The observed patterns of intra-regional concordance do not depart from random values with the exception of the Gulf region where the internal concordance value of 0.20 is significantly below that observed under the null hypothesis of random spatial patterning of rank changes. Put another way, the member states of the Gulf region exchange ranks more frequently with one another than what would be expected by random chance.

In contrast to the intra-regional concordance results, interregional rank mobility departs from randomness more frequently. For example, states from the South and North regions never experience pairwise exchange of ranks leading to significant concordance (lack of mobility) over this period. This reflects the well-known gap between the incomes of states located in the northern and southern borders of Mexico. At the same time, the North and Center regions also display

rank separation. Alongside these instances of rank concordance, there are two pairs of regions that exhibit significant interregional exchange mobility, these are the Center and Gulf, and the Center-N and North region. The case of the Center region thus illustrates that the decomposition can illuminate meso-level pairwise interregional dynamics that may be masked by the global mobility measure and not considered by the location specific indicators. Thus the interregional and intraregional mobility decomposition provides a useful complement to the global and local analytics.

[Table 5 about here.]

5. CONCLUSION

This article has introduced a family of local indicators of mobility association that provide a number of new perspectives on space-time dynamics. First, the LIMAs are directly linked to previously developed global indicators of spatial concordance that identify hot-spots, and cold-spots, of spatial change, together with locations that deviate from the overall general pattern of space-time concordance. Second, the additive decomposition of the LIMAs permits the development of a meso-level analytic to examine whether the overall space-time concordance is driven by interregional or intraregional concordance. That is, are groups of observations (regions) displaying space-time dynamics distinct from the global pattern? This adds an important dynamic complement to the work on static decomposition of spatial inequality into its interregional and intraregional parts.

The initial application of these measures to the case study of Mexican state income dynamics over the 1940-2000 period suggests that the LIMAs can provide new insights on regional income distribution dynamics. At the same time, this is an initial foray into the LIMAs and much work remains to be done. The LIMA statistics are designed to detect hot-spots of space-time concordance and uncover interesting patterns in spatial pattern evolution. These are some of the goals of exploratory space-time methods, which, in turn lead naturally to questions about the processes may be responsible for the patterns uncovered. From a policy evaluation perspective there has been a resurgence of interest in new methods to examine the impacts of “trickle-down” economic policies on inequality and mobility (e.g. Bourguignon, 2011), and the LIMA’s offer a spatial lens on these distributional questions. More broadly, the development of spatially explicit theories of economic growth that relies on the LIMA statistics to identify leading and lagging regions (LeSage

and Reed, 1990), the role of labor migration and changes in industrial composition (Crescenzi et al., 2012), and to address the question of whether regional economic growth is competitive or cooperative between neighboring regions (Chung and Hewings, 2015) are just a selection among the numerous future avenues for confirmatory work that the new measures can afford.

From a more methodological perspective there are also several key areas for future research. Thus far inference on the LIMAs has been based on conditional random spatial permutations which provides one approach to assessing the statistical significance of the indicators. Computational challenges associated with the global space-time concordance measure have been addressed (Rey, 2014) but need to be revisited in the local case since now conditional permutations are required. The theoretical sampling distributions of the LIMA family also need to be examined. This is particularly important as the LIMAs are a specific case of a local statistic, and thus face the same challenges shared by all local statistics. These include the issues of multiple comparisons, the lack of independence between the individual LIMAs, the distribution of the local statistics in the presence of global space-time concordance, and the sensitivity of the statistic to the choice of spatial weights matrix. Additionally, the developing composite measures of spatial dynamics that combine changes in a global, and local, spatial autocorrelation statistics with the LIMAs presented here is a promising direction for future research.

As the LIMAs are based on ranks the issues associated with the shift from an interval to ordinal measurement scale raises the question of a trade-off between a potential loss of power and a gain of generality. The generality arises from the relaxation of a number of potentially restrictive assumptions underlying traditional correlation statistics. For example, in a space-time context the analysis of change in absolute values of some series can be problematic, as in the case of remote sensing data where direct comparison of illumination data from two different periods is difficult without rank normalization of the data (Nelson et al., 2005). Similarly, rank distributions are robust to extreme outliers that can have major impacts on interval correlation statistics. Moreover, there is some evidence to suggest that the power of rank statistics can actually be quite high (Kendall, 1962, p 166) so the trade-off between increased generalization and loss of power may not be as great as first thought.

Although the LIMAs have their origin in studying regional income mobility, the analytics suggested in this article are appropriate for a wide array of phenomena measured in space-time.

The avalanche of new types of spatio-temporal data associated with streaming sources (i.e., sensors, geographical positioning systems, imagery, cell phones, etc.) appears to be an ideal domain for the use of the LIMAs to identify space-time clustering, emergent properties, as well as rigidity and inertia in space-time patterns. The LIMAs have an interesting property that they can be efficiently updated when new data become available unlike other space-time correlation measures that would require complete recalculation.

Finally, while the current application relied on polygon data to illustrate the LIMAs and their properties, the approach can easily be extended to any type of spatial support where neighbor relationships between observational units can be defined. For example, LIMAs could be applied to the analysis of network constrained phenomena, such as traffic flows, or to marked point patterns.⁴ Irrespective of the specific spatial support, the LIMAs could also be employed as part of new data-driven approaches to delineate regions and/or to detect changes in region definitions over time.

REFERENCES

- Anselin, L. (1995). Local indicators of spatial association-LISA. *Geographical Analysis*, 27(2):93–115.
- Anselin, L. and Rey, S. J. (2014). *Modern spatial econometrics in practice: A guide to GeoDa, GeoDaSpace and PySAL*. GeoDa Press.
- Aroca, P., Bosch, M., and Maloney, W. F. (2005). Spatial dimensions of trade liberalization and economic convergence: Mexico 1985–2002. *The World Bank Economic Review*, 19(3):345–378.
- Beenstock, M. and Felsenstein, D. (2007). Mobility and mean reversion in the dynamics of regional inequality. *International Regional Science Review*, 30(4):335–361.
- Bigman, D. and Srinivasan, P. (2002). Geographical targeting of poverty alleviation programs: methodology and applications in rural India. *Journal of Policy Modeling*, 24(3):237–255.
- Bourguignon, F. (2011). Non-anonymous growth incidence curves, income mobility and social welfare dominance. *The Journal of Economic Inequality*, 9(4):605–627.

⁴I thank the anonymous referees for these suggestions.

-
- Chetty, R., Hendren, N., Kline, P., and Saez, E. (2014). Where is the land of opportunity? The geography of intergenerational mobility in the United States. Technical report, National Bureau of Economic Research.
- Chung, S. and Hewings, G. J. (2015). Competitive and complementary relationship between regional economies: a study of the Great Lake States. *Spatial Economic Analysis*, 10(2):205–229.
- Cramer, C. (2003). Does inequality cause conflict? *Journal of International Development*, 15(4):397–412.
- Crescenzi, R., Rodríguez-Pose, A., and Storper, M. (2012). The territorial dynamics of innovation in China and India. *Journal of Economic Geography*, 12(5):1055–1085.
- Cuadrado-Roura, J. R. (2009). *Regional policy, economic growth and convergence: lessons from the Spanish case*. Springer Verlag.
- Esquivel, G. (1999). Convergencia regional en México, 1940-1995. *El trimestre económico*, (264):725.
- Fields, G. (2010). Does income mobility equalize longer-term incomes? New measures of an old concept. *Journal of Economic Inequality*, 8(4):409–427.
- Formby, J., Smith, W., and Zheng, B. (2004). Mobility measurement, transition matrices and statistical inference. *Journal of Econometrics*, 120(1):181–205.
- Hammond, G. W. and Thompson, E. (2006). Convergence and mobility: Personal income trends in US metropolitan and nonmetropolitan regions. *International Regional Science Review*, 29(1):35–63.
- Jalan, J. and Ravallion, M. (1998). Are there dynamic gains from a poor-area development program? *Journal of Public Economics*, 67(1):65–85.
- Kanbur, S. and Venables, A. (2005). *Spatial inequality and development*. Oxford University Press, USA.
- Kendall, M. G. (1962). *Rank correlation methods*. Griffin, London, 3rd edition.
- Le Gallo, J. (2004). Space-time analysis of GDP disparities across European regions: a Markov chains approach. *International Regional Science Review*, 27(2):138–163.
- LeSage, J. and Reed, J. (1990). Testing criteria for determining leading regions in wage transmission models testing criteria for determining leading regions in wage transmission models testing

-
- criteria for determining leading regions in wage transmission models. *Journal of Regional Science*, 30(1):37–50.
- Maasoumi, E. (1998). On mobility. *Handbook of applied economic statistics*, pages 119–175.
- Maasoumi, E., Racine, J., and Stengos, T. (2007). Growth and convergence: A profile of distribution dynamics and mobility. *Journal of Econometrics*, 136(2):483–508.
- Magrini, S. (1999). The evolution of income disparities among the regions of the European Union. *Regional Science and Urban Economics*, 29(2):257–281.
- Nelson, T., Wilson, H., Boots, B., and Wulder, M. (2005). Use of ordinal conversion for radiometric normalization and change detection. *International Journal of Remote Sensing*, 26(3):535–541.
- Partridge, M. D. (1997). Is inequality harmful for growth? Comment. *The American Economic Review*, pages 1019–1032.
- Piketty, T. (2014). *Capital in the Twenty-first Century*. Harvard University Press.
- Quah, D. T. (1996a). Empirics for economic growth and convergence. *European Economic Review*, 40(6):1353–1375.
- Quah, D. T. (1996b). Twin peaks: Growth and convergence in models of distribution dynamics. *The Economic Journal*, 106:1045–1055.
- Rey, S. J. (2001). Spatial empirics for economic growth and convergence. *Geographical Analysis*, 33(3):195–214.
- Rey, S. J. (2004). Spatial analysis of regional income inequality. In Goodchild, M. and Janelle, D., editors, *Spatially Integrated Social Science: Examples in Best Practice*, pages 280–299. Oxford University Press, Oxford.
- Rey, S. J. (2014). Fast algorithms for a space-time concordance measure. *Computational Statistics*, 29(3-4):799–811.
- Rey, S. J. (2016). Bells in space: The spatial dynamics of US interpersonal and interregional income inequality. *International Regional Science Review*, doi:10.1177/0160017615614899.

-
- Rey, S. J. and Anselin, L. (2007). PySAL: A Python library of spatial analytical methods. *The Review of Regional Studies*, 37(1):5–27.
- Rey, S. J. and Montouri, B. D. (1999). U.S. regional income convergence: A spatial econometric perspective. *Regional Studies*, 33(2):145–156.
- Rey, S. J. and Sastré-Gutiérrez, M. L. (2010). Interregional inequality dynamics in Mexico. *Spatial Economic Analysis*, 5(3):277–298.
- Schluter, C. (1998). Statistical inference with mobility indices. *Economics letters*, 59(2):157–162.
- Schorrocks, A. (1978). Income inequality and income mobility. *Journal of Economic Theory*, 19:376–393.
- Shorrocks, A. and Wan, G. (2005). Spatial decomposition of inequality. *Journal of Economic Geography*, 5(1):59–81.
- Stiglitz, J. (2012). *The price of inequality*. Penguin UK.
- The Economist (2011). Regional inequity: The gap between many rich and poor regions widened because of the recession. http://www.economist.com/node/18332880?story_id=18332880.
- Webber, D., White, P., and Allen, D. (2005). Income convergence across US States: An analysis using measures of concordance and discordance. *Journal of Regional Science*, 45(3):565–589.

SERGIO REY is a Professor in the School of Geographical Sciences and Urban Planning at Arizona State University, Tempe, AZ 85287. E-mail: srey@asu.edu. His research interests include spatio-temporal data analysis, geocomputation, geovisualization, regional inequality dynamics, open science, and regional science.

LIST OF FIGURES

1	Global Indicator of Rank Mobility: Case I	26
2	Global Indicator of Rank Mobility: Case II	27
3	Relative per capita gross domestic product by state 1940-2000. Legend values are upper bound of each quintile.	28
4	Spaghetti Plot, relative incomes Mexican States 1940-2000	29
5	Rank changes and cumulative absolute rank changes, relative per capita gross domestic product by state 1940-2000. Legend values are upper bound of each quintile.	30
6	Mexican states and regions	31

1	2	5	6
3	4	7	8
9	10	13	14
11	12	15	16

(a) Ranks period t_0

1	2	5	6
3	4	7	8
9	10	16	15
11	12	14	13

(b) Ranks period t_1

0	0	1	1
0	0	1	1
2	2	3	3
2	2	3	3

(c) Regimes

Figure 1: Global Indicator of Rank Mobility: Case I

1	2	5	6
3	4	7	8
9	10	13	14
11	12	15	16

(a) Ranks period t_0

5	6	1	2
7	8	3	4
13	14	9	10
15	16	11	12

(b) Ranks period t_1

0	0	1	1
0	0	1	1
2	2	3	3
2	2	3	3

(c) Regimes

Figure 2: Global Indicator of Rank Mobility: Case II

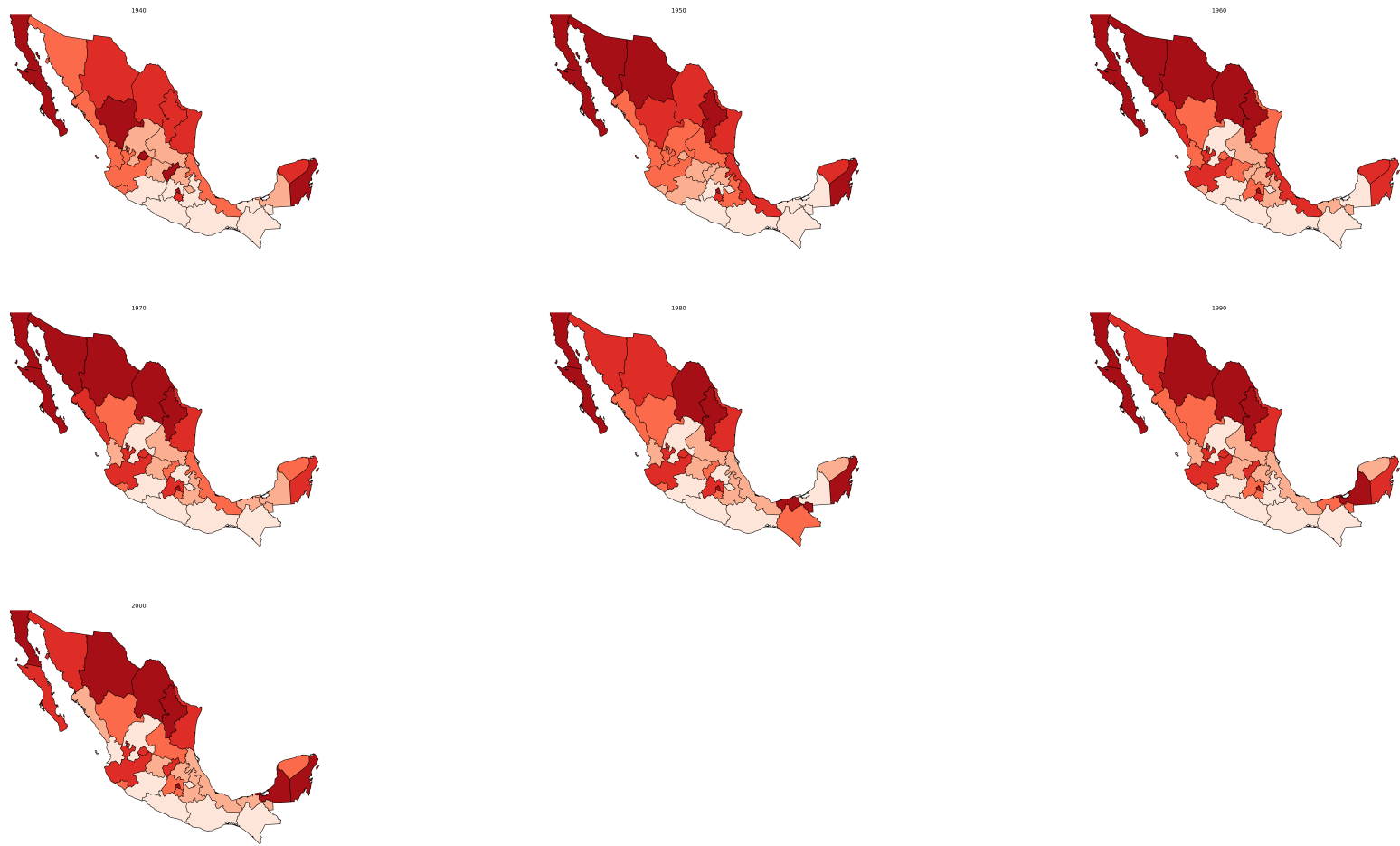


Figure 3: Relative per capita gross domestic product by state 1940-2000. Legend values are upper bound of each quintile.

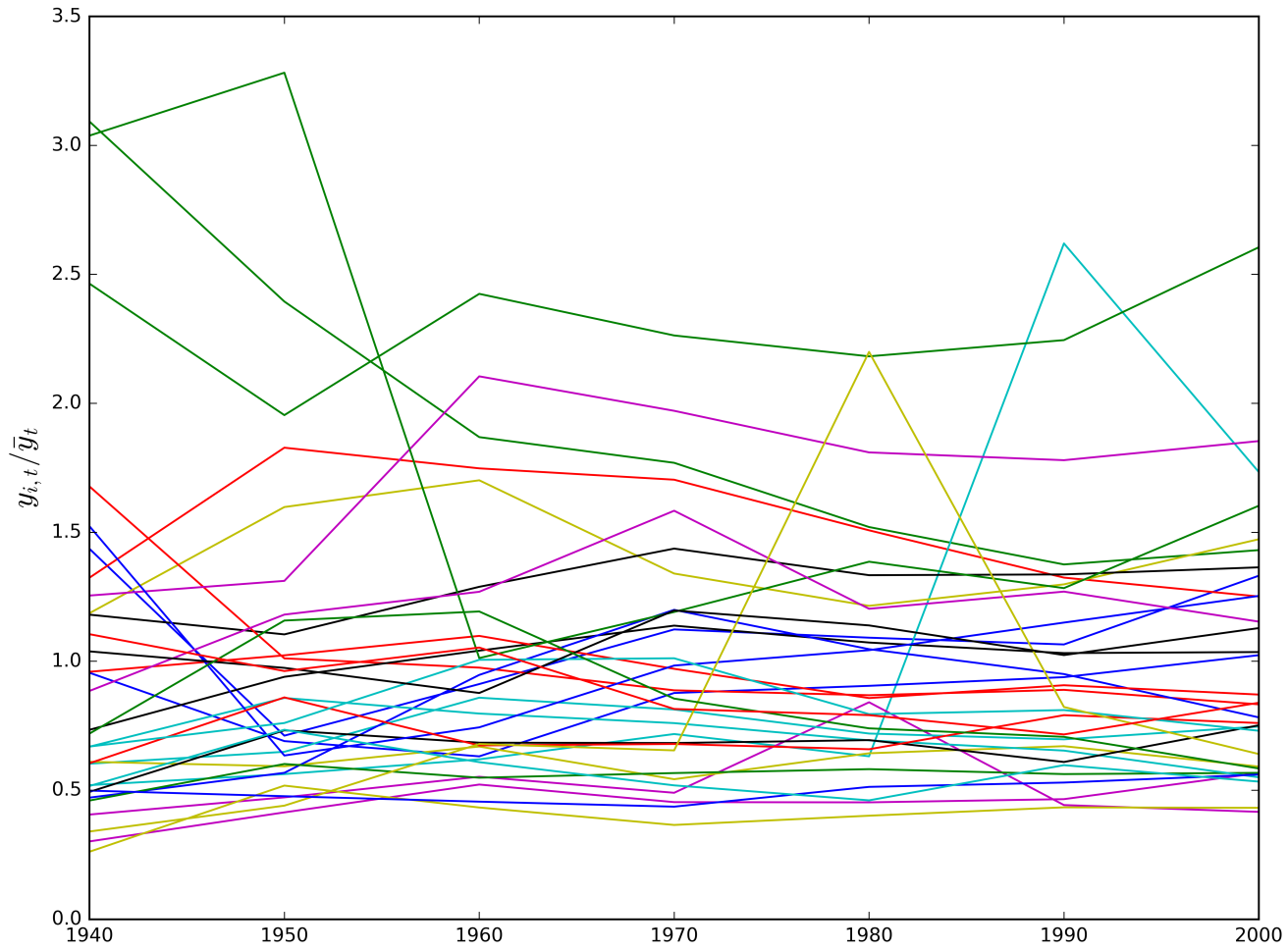


Figure 4: Spaghetti Plot, relative incomes Mexican States 1940-2000

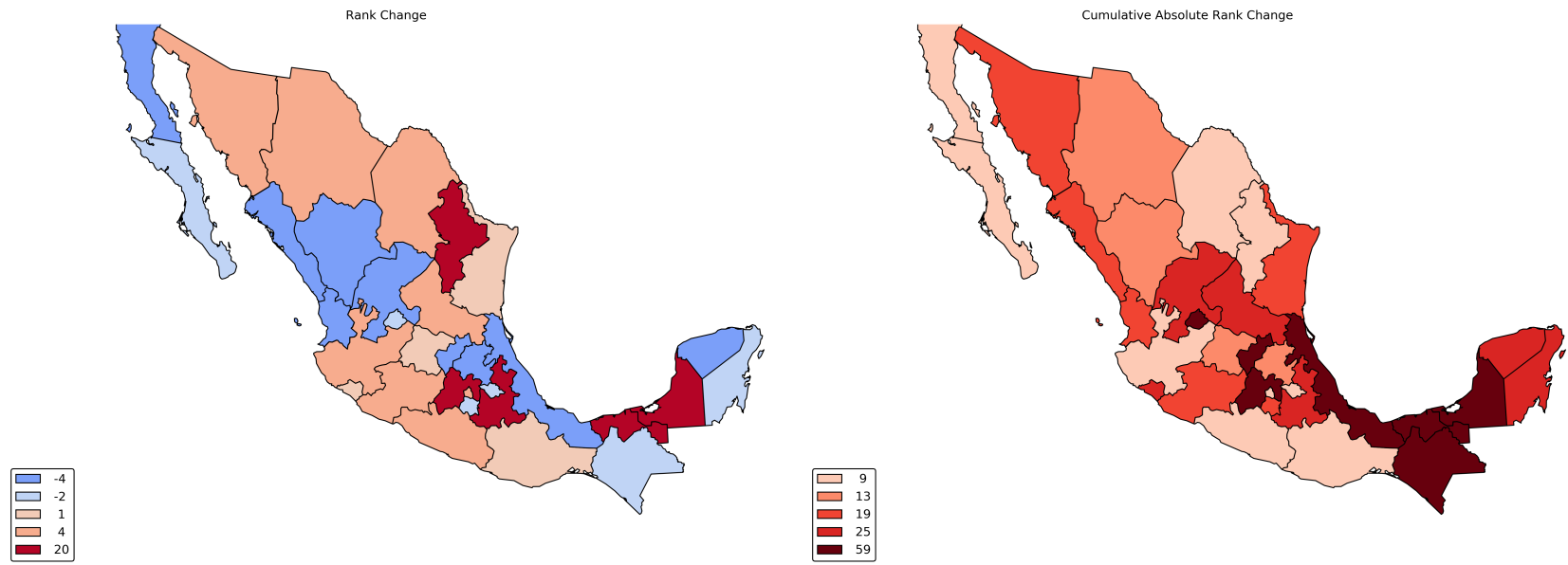


Figure 5: Rank changes and cumulative absolute rank changes, relative per capita gross domestic product by state 1940-2000. Legend values are upper bound of each quintile.



(a) Mexican States



(b) Mexican regions after Esquivel (1999)

Figure 6: Mexican states and regions

LIST OF TABLES

1	Global Concordance and Spatial Autocorrelation	33
2	Location specific τ_i . Bold values indicate significant LISA statistics for the associated τ_i	34
3	Neighbor set Local Indicators of Mobility Association: $\tilde{\tau}_i$. Bold values are statistically significant at $p = 0.05$	35
4	Neighborhood set Local Indicators of Mobility Association: $\tilde{\tilde{\tau}}_i$. Bold values are statistically significant at $p = 0.05$	36
5	Inter and Intra-regional Concordance Decomposition 1940-2000. Values on the diagonal are the intraregional concordance indicator, off-diagonals are interregional concordance indicators. Bold indicates a significant concordance value.	37

Year	τ_w	$E[\tau_w]$	p-value	I	$E[I]$	p-value
1940	0.397	0.658	0.005	-0.019	-0.034	0.390
1950	0.492	0.699	0.009	0.035	-0.035	0.230
1960	0.651	0.763	0.047	0.327	-0.026	0.015
1970	0.714	0.752	0.223	0.561	-0.032	0.001
1980	0.683	0.701	0.307	0.258	-0.028	0.026
1990	0.810	0.820	0.333	0.213	-0.035	0.042
2000	-	-	-	0.160	-0.037	0.071

Table 1: *Global Concordance and Spatial Autocorrelation*

State	τ_i 40-50	τ_i 50-60	τ_i 60-70	τ_i 70-80	τ_i 80-90	τ_i 90-00
Aguascalientes	-0.03	0.61	0.61	0.81	0.74	0.81
Baja California	0.94	0.81	1.00	0.94	0.87	0.87
Baja California Sur	0.81	0.87	1.00	0.94	0.81	0.74
Campeche	0.74	0.81	0.74	0.68	-0.68	0.87
Chiapas	0.94	0.74	0.94	0.29	0.16	0.94
Chihuahua	0.74	0.87	0.87	0.81	0.81	0.74
Coahuila	0.68	0.81	0.87	0.81	0.74	0.87
Colima	0.42	0.61	0.48	0.74	0.87	0.94
Distrito Federal	1.00	0.87	1.00	0.94	0.87	0.94
Durango	0.55	0.81	0.61	0.74	0.81	0.87
Guanajuato	0.74	0.61	0.87	0.87	0.81	0.74
Guerrero	0.94	0.87	1.00	0.94	0.94	0.81
Hidalgo	0.68	0.68	0.81	0.81	0.74	0.87
Jalisco	0.74	0.81	0.61	0.81	0.74	0.94
Mexico	0.81	0.29	0.55	0.68	0.81	0.74
Michoacan	0.74	0.68	0.81	0.87	0.87	0.87
Morelos	0.55	0.94	0.48	0.74	0.81	0.94
Nayarit	0.68	0.68	0.87	0.81	0.68	0.74
Nuevo Leon	0.74	0.74	1.00	0.94	0.87	0.94
Oaxaca	0.74	0.74	1.00	1.00	1.00	0.94
Puebla	0.55	0.61	0.87	0.74	0.68	0.61
Quertaro	-0.16	0.68	0.61	0.87	0.61	0.81
Quintana Roo	0.94	0.29	0.61	0.61	0.74	0.74
San Luis Potosi	0.61	0.48	0.81	0.81	0.55	0.81
Sinaloa	0.68	0.74	0.61	0.61	0.87	0.68
Sonora	0.48	0.87	0.87	0.74	0.87	0.87
Tabasco	0.94	0.42	0.81	-0.55	-0.10	0.68
Tamaulipas	0.61	0.68	0.48	0.81	0.68	0.94
Tlaxcala	0.74	0.74	1.00	0.87	0.87	0.81
Veracruz	0.42	0.87	0.35	0.81	0.81	0.81
Yucatan	0.61	0.81	0.42	0.81	0.81	0.68
Zacatecas	0.61	0.42	0.94	0.87	0.81	0.81

Table 2: Location specific τ_i . Bold values indicate significant LISA statistics for the associated τ_i .

State	$\tilde{\tau}_r$ 40-50	$\tilde{\tau}_r$ 50-60	$\tilde{\tau}_r$ 60-70	$\tilde{\tau}_r$ 70-80	$\tilde{\tau}_r$ 80-90	$\tilde{\tau}_r$ 90-00
Aguascalientes	-0.20	0.20	0.60	1.00	0.60	0.60
Baja California	1.00	0.60	1.00	1.00	1.00	0.60
Baja California Sur	1.00	1.00	1.00	1.00	1.00	1.00
Campeche	1.00	0.50	0.50	0.50	-1.00	1.00
Chiapas	0.33	-0.33	0.33	0.33	-0.33	0.33
Chihuahua	0.60	0.60	0.20	0.60	1.00	0.20
Coahuila	0.60	0.60	0.20	0.60	1.00	0.60
Colima	-0.50	1.00	0.50	0.50	1.00	1.00
Distrito Federal	1.00	1.00	1.00	1.00	1.00	1.00
Durango	1.00	1.00	0.20	1.00	1.00	1.00
Guanajuato	0.20	0.20	0.60	1.00	0.60	1.00
Guerrero	0.33	0.33	1.00	1.00	0.33	1.00
Hidalgo	0.33	1.00	1.00	1.00	0.33	0.33
Jalisco	0.50	1.00	1.00	1.00	1.00	1.00
Mexico	1.00	1.00	1.00	1.00	1.00	1.00
Michoacan	1.00	0.33	0.33	0.33	0.33	1.00
Morelos	1.00	1.00	1.00	1.00	1.00	1.00
Nayarit	0.00	0.50	0.50	1.00	1.00	1.00
Nuevo Leon	0.60	0.20	1.00	1.00	1.00	1.00
Oaxaca	-0.33	-0.33	1.00	1.00	1.00	0.33
Puebla	-0.33	1.00	1.00	1.00	0.33	0.33
Quertaro	-0.60	0.20	0.20	1.00	0.60	0.60
Quintana Roo	1.00	0.00	0.00	0.50	0.00	1.00
San Luis Potosi	0.20	-0.20	1.00	1.00	0.60	1.00
Sinaloa	0.00	0.50	1.00	0.50	1.00	1.00
Sonora	0.20	0.60	0.20	0.20	1.00	1.00
Tabasco	1.00	0.50	0.50	-1.00	0.00	0.50
Tamaulipas	0.60	1.00	1.00	1.00	1.00	1.00
Tlaxcala	0.33	1.00	1.00	1.00	1.00	1.00
Veracruz	0.50	0.50	0.50	0.00	0.50	1.00
Yucatan	0.50	0.50	0.50	0.00	0.50	0.50
Zacatecas	-0.20	-0.20	1.00	1.00	1.00	1.00

Table 3: Neighbor set Local Indicators of Mobility Association: $\tilde{\tau}_i$. Bold values are statistically significant at $p = 0.05$.

State	$\tilde{\tau}_r$ 40-50	$\tilde{\tau}_r$ 50-60	$\tilde{\tau}_r$ 60-70	$\tilde{\tau}_r$ 70-80	$\tilde{\tau}_r$ 80-90	$\tilde{\tau}_r$ 90-00
Aguascalientes	0.07	0.20	0.60	1.00	0.73	0.87
Baja California	0.60	0.60	0.60	0.73	1.00	0.73
Baja California Sur	0.20	0.80	0.80	0.80	1.00	1.00
Campeche	0.80	0.40	0.40	0.00	0.00	0.80
Chiapas	0.33	0.00	0.67	0.67	0.33	0.67
Chihuahua	0.60	0.60	0.60	0.73	1.00	0.73
Coahuila	0.60	0.60	0.60	0.73	1.00	0.73
Colima	0.20	0.80	0.80	0.80	1.00	1.00
Distrito Federal	1.00	1.00	1.00	1.00	1.00	1.00
Durango	0.07	0.20	0.60	1.00	0.73	0.87
Guanajuato	0.07	0.20	0.60	1.00	0.73	0.87
Guerrero	0.33	0.00	0.67	0.67	0.33	0.67
Hidalgo	0.33	1.00	1.00	1.00	0.67	0.67
Jalisco	0.20	0.80	0.80	0.80	1.00	1.00
Mexico	1.00	1.00	1.00	1.00	1.00	1.00
Michoacan	0.33	0.00	0.67	0.67	0.33	0.67
Morelos	0.33	1.00	1.00	1.00	0.67	0.67
Nayarit	0.20	0.80	0.80	0.80	1.00	1.00
Nuevo Leon	0.60	0.60	0.60	0.73	1.00	0.73
Oaxaca	0.33	0.00	0.67	0.67	0.33	0.67
Puebla	0.33	1.00	1.00	1.00	0.67	0.67
Quertaro	0.07	0.20	0.60	1.00	0.73	0.87
Quintana Roo	0.80	0.40	0.40	0.00	0.00	0.80
San Luis Potosi	0.07	0.20	0.60	1.00	0.73	0.87
Sinaloa	0.20	0.80	0.80	0.80	1.00	1.00
Sonora	0.60	0.60	0.60	0.73	1.00	0.73
Tabasco	0.80	0.40	0.40	0.00	0.00	0.80
Tamaulipas	0.60	0.60	0.60	0.73	1.00	0.73
Tlaxcala	0.33	1.00	1.00	1.00	0.67	0.67
Veracruz	0.80	0.40	0.40	0.00	0.00	0.80
Yucatan	0.80	0.40	0.40	0.00	0.00	0.80
Zacatecas	0.07	0.20	0.60	1.00	0.73	0.87

Table 4: Neighborhood set Local Indicators of Mobility Association: $\tilde{\tau}_i$. Bold values are statistically significant at $p = 0.05$.

	Capital	Center	Center-N	Gulf	North	Pacific	South
Capital	1.00	0.25	0.50	0.60	0.83	0.60	1.00
Center	0.25	0.33	0.50	0.30	0.92	0.40	0.75
Center-N	0.50	0.50	0.60	0.40	0.39	0.53	0.83
Gulf	0.60	0.30	0.40	0.20	0.40	0.28	0.80
North	0.83	0.92	0.39	0.40	0.60	0.73	1.00
Pacific	0.60	0.40	0.53	0.28	0.73	0.80	0.80
South	1.00	0.75	0.83	0.80	1.00	0.80	0.33

Table 5: *Inter and Intraregional Concordance Decomposition 1940-2000. Values on the diagonal are the intraregional concordance indicator, off-diagonals are interregional concordance indicators. Bold indicates a significant concordance value.*